

Full Length Research Paper

# Different polarised topographic synthetic aperture radar (TOPSAR) bands for shoreline change mapping

Maged Marghany\* and Mazlan Hashim

Institute of Geospatial Science and Technology (INSTEG), Universiti Teknologi Malaysia 81310 UTM, Skudai, Johore Bahru, Malaysia.

Accepted 17 September, 2010

**This study introduced a new approach for coastal erosion and sedimentation monitoring. In doing so, the airborne topographic synthetic aperture radar (TOPSAR) polarized data is used with the conventional techniques of mapping shoreline rate changes, which is based on the estimation of historical vector layers. The main problem for shoreline identification is raised up due to speckles impact. Therefore, the speckle reductions are performed by using an adaptive filter algorithm to identify the coastline edge morphology. In this context, Lee algorithm, combination of linear contrast, Gaussian and histogram equalization enhancement is used. Thus the manual vector layer digitizing is applied to extract the coastline for the different polarized bands. Further, the accuracy assessment is determined based on the statistical analysis of T-test. Indeed, T-test is used to determine the significant distinction between the TOPSAR different polarized bands. For more precisely, SPOT satellite data are used with near real time *in situ* measurements to determine appropriate band for shoreline change estimation. The results show that the  $C_{VV}$  band is performed better than other bands with root mean square error of  $\pm 0.9$  m and  $r^2$  of 0.73. This confirms with T-test in which there is a major difference between C and L bands.**

**Key words:** Air borne topographic synthetic aperture radar,  $C_{VV}$ ,  $L_{HH}$ ,  $L_{VV}$  band, polarization, SPOT satellite data, statistical T-test.

## INTRODUCTION

The study of shoreline change is barely task. In fact, it is difficult to define the accurate geographical location of shoreline due to the complex dynamics's interaction between the ocean and coastline. There are, conversely, many contrast shoreline definitions. The classical definition states that the shoreline is a boundary zone between land and sea. This definition in practice, nevertheless, is complex to concern. According to Boak and Turner (2005), the shoreline position in reality varies consistently since dynamic sediment movements in the littoral zone. Particularly, the dynamic water level's changes at the coastal boundary play a great role for inaccurate identification of exact shoreline positions.

Therefore, Boak and Turner (2005), imposed a proxy to

define a true shoreline position. They reported that the common shoreline proxy has been a subject of much debat is "the high water line" (Anders and Byrnes, 1991; El-Raey et al., 1995; Frihy et al., 1995). In contrast, Maged (2001) and (2003) argued to use the high water line or low water line as indicator for shoreline position specially in tropical sandy beach. This argument has confirmed with studies of Pajak and Leatherman, (2002) and Stockdon et al. (2002). Boak and Turner (2005), consequently, reported that this terminology introduces tremendous source of potential uncertain. In this context, the wet/dry line changes dynamically based on tidal periodic cycle. It is considered to be the rising maximum runup on a flooding tide, while landward extent of the falling wet beach during tidal ebb (Boak and Turner, 2005). Thus, Maged (2001 and 2003) identifies the shoreline position as an end of vegetation line in tropical sandy beach.

Frighy et al. (1995), El-Raey et al.(1995) and Teodoro

\*Corresponding author. E-mail: [maged@utm.my](mailto:maged@utm.my), [magedupm@hotmail.com](mailto:magedupm@hotmail.com).

et al. (2009) used different historical data of Landsat MSS and Landsat TM satellite imagery, aerial photography and topographic maps for coastal erosion studies. Most of these studies found an unrealistic high rate of erosion of more than 50 months/year. Frighy et al. (1995) and El-Raey et al. (1995), for instance, estimated the rate of erosion in the Nile Delta to be  $-70.8$  months/year. Yet, if this rate is accurate, it would have smashed of all the infrastructures, such as roads and bridges near the coastal waters. Additionally, Frighy et al. (1995) and El-Raey et al. (1995) declared there is a significant relation between shoreline change, estimated from Landsat TM, aerial photography and ground surveys with a correlation coefficient ( $r$ ) of 0.93. In contrary, Maged (2001 and 2003) argued the studies of Frighy et al. (1995) and El-Raey et al. (1995). Maged (2001 and 2003) claimed that both studies did not show accurate significant relationship between remote sensing data and ground survey. In fact, the ground survey did not take in real or near real time of satellite overpass. Further, a significant statistical test such as ANOVA or the t-test have not been performed. In addition, the low resolution of the Landsat data (30 m) only justifies its use in coastal erosion studies with changes that are larger than this pixel size. As a matter of fact, the resolution of this sensor is unable to capture beach profiles at a width less than the pixel size ( $< 30$  m). The high resolution of SPOT PAN (10 m) and radar data such as from ERS-1 (12.5 m), RADARSAT (12.5 m) and AIRSAR/TOPSAR (ca. 10 m) enables us to solve this type of problem.

The operational use of synthetic aperture radar (SAR) on coastal studies is of interest for diversity of end users. In this context, 34% of the world's coasts are exposed to critical risk of degradation. Therefore, the critical problem that can arise from using SAR data for shoreline change monitoring the speckle. In this context, Lee and Jurkevich (1990) introduced a new approach based on an edge-tracing algorithm to determine an exact position of shoreline. However, they stated that sea state conditions as long as the impact the SAR signal backscatter from a sea surface, it can cause too equal or overwhelm backscatter from coastal land areas. Further, Yu and Acton (2004) utilized speckle-reducing anisotropic diffusion tools to delineate the shoreline from space borne polarimetric SAR imagery. Moreover, Baghdadi et al. (2004) compared between ERS-1 and RADARSAT-1 SAR data for shoreline mapping. They found that RADARSAT-1 SAR has a better performance due to its wide incidence angles. Thus, Liu et al. (2004) argued that the absolute accuracy is influenced not only by the coastline extraction method but, also by the georeferencing accuracy of the source images. To derive a coastline, in consequence, with precise absolute geographical coordinates and correct geometric shape the, source images used to extract the coastline must be geocoded and orthorectified before applying coastline extraction algorithms. Recently, Kim et al. (2007) proposed a

new approach for mapping shoreline change based on radar frequency. They pointed out in the intertidal areas, the Bragg scattering of resonant Bragg's waves is a function of wavelength. They, consequently, concluded that SAR data with shorter wavelength are appropriate for shoreline extraction. At present, Shu et al. (2010) implemented narrow band level set segmentation approach for semi-automatic detection of shoreline using RADARSAT-2 SAR fine mode data. Nevertheless, Gens (2010) argued that the disadvantage of these methods is, therefore the, lack of shoreline positional accuracy.

Using the  $C_{VV}$  image to map the coastline change could consider as imperfect study as the research limits to one band. Topographic synthetic aperture radar (TOPSAR) system is capable of simultaneously collecting HH and VV polarizations in three frequencies (P-, L- and C-bands) in one mapping. Coastline change detection using the TOPSAR data is done by Maged (2000) and (2001) on C-band with VV polarization along the coast of Kuala Terengganu. The C-VV polarized image was compared to the real time ground data and historical ship observation data to extract the change rate along the Kuala Terengganu coast. Another study to determine which of the polarized L- or C-band TOPSAR data is more suitable for wave refraction detection is been carried out by Maged (1999), showed that TOPSAR L-band is more useful to investigate the wave refraction patterns.

The contribution of this study is to use multi-TOPSAR polarization data for mapping shoreline changes rate with integration of SPOT satellite data. Indeed, SPOT pixel resolution of 10 m is similar as TOPSAR polarization data. We hypothesized that TOPSAR can be utilized to detect the accurate position of shoreline. In addition, different polarization band in radar imaging having dissimilar backscatter and wavelengths, in which it provides contradictory information in shoreline change mapping. On other words, there is a significant difference between unlike TOPSAR polarized bands in mapping shoreline changes rate. The main objective of this study is to reveal the proper TOPSAR polarized bands for shoreline change rate mapping. In doing so, C and L bands with VV and HH polarization are considered.

## RESEARCH METHODS

### Study area

The study area is located in the South China Sea along the coastal water of Kuala Terengganu, eastern coast of Peninsular Malaysia. It is located between  $5^{\circ}20'$  N to  $5^{\circ}27'$  N and  $103^{\circ}5'$  E to  $103^{\circ}9'$  E. This area lies on the equatorial region, and is affected by monsoon winds (Maged, 2001). Indeed during the Northeast monsoon period, the strong storm and wave height of 4 m can cause erosion (Maged, 2001). The 20 km stretches of coastal along the Kuala Terengganu shoreline composed of sandy beach, the kind of most frequently eroded region. The significant source of sand was from Terengganu River. Some sediment loses to the continental shelf due to the complex movements of waves approached from the

north direction (Maged, 2003).

**Data acquisition**

**TOPSAR data**

The remote sensing data used in this study categories into (i) microwave, (ii) optical satellite and (iii) aerial photography data (Table 1). The microwave data are airborne data while the optical data are multispectral SPOT satellite data. The NASA JPL (Jet Propulsion Laboratory) airborne TOPSAR data was acquired on 3rd December, 1996 related to the ASIAN PACRIM research. The data was acquired along the Kuala Terengganu region between 5°20' N to 5°27' N to 103°5' E to 103°9' E. TOPSAR data acquired in this study were derived from the Jet Propulsion Laboratory (JPL) airborne TOPSAR data. TOPSAR is a NASA/JPL multi-frequency radar imaging system aboard a DC-8 aircraft and operated by NASA's Ames Research Center at Moffett Field, USA. TOPSAR data are fully polarimetric SAR data acquired with HH-, VV-, HV- and VH-polarized signals from 5 x 5 m pixels, recorded for three wavelengths: C band (5 cm), L band (24 cm) and P band (68 cm). The full set of C-band and L-band have linear polarizations (HH, VV, HV), phase differences (HHVV), and circular polarizations (RR, RL). In addition, the TOPSAR sensor uses two antennas to receive the radar backscatter from the surface. The difference in arrival times of the return signals at the two antenna was converted into a modulo  $-2\pi$  phase difference. Further, TOPSAR data with C-band provides digital elevation model with rms error in elevation ranging from about 1 m in the near range to greater than 3 m in the far range. A further explanation of TOPSAR data acquisition is given by Melba et al. (1999). This study utilizes both  $C_{VV}$ ,  $L_{VV}$  and  $L_{HH}$  bands for 2-D shoreline change rate mapping because of the widely known facts of the good interaction of VV and HH polarization to oceanographic physical elements such as ocean wave, surface current features, etc. Elaboration of such further explanation can be found in (Melba et al., 1999; Maged and Mazlan, 2006; Maged et al., 2010).

To identify the shoreline position in TOPSAR polarised data, Lee algorithm used with window kernal size of 3 x 3 which is suitable for shoreline width less than 10 m. According to Maged (2002) and Maged et al. (2010), Lee algorithm smooths all pixel edges are where edges of the edge-pixels are replicated to give sufficient data. In this study, Lee algorithm for combined additive and multiplicative noise is used. Indeed, Lee algorithm is primarily used on radar data to remove high frequency noise (speckle) while preserving shoreline edges (Maged et al., 2010).

**SPOT satellite data**

Three bands of SPOT multi-spectral satellite are selected: (i) green (0.50 - 0.59  $\mu\text{m}$ ); (ii) red (0.61 - 0.68  $\mu\text{m}$ ); and (iii) near IR (0.79 - 0.89  $\mu\text{m}$ ). This data acquired in 18th December, 2003. In the near infrared (IR) band, the land-water interface is clearly defined as the water absorbed the radiation energy and, thereby, contributed nearly no energy returns. As for the land features, the radiation reflects according to the nature of the properties of the materials it hits (Figure 1). Following Guariglia et al. (2006), the shoreline position is detect by the following formula:

$$\text{If Near IR}/(\text{Green}-\text{Red}) < 1 \text{ then } 255 \text{ else } 0 \text{ (1)}$$

**Remote sensing data geocoding**

The topographic maps were scanned and loaded into PCI

**Table 1.** Remote sensing data used in this study.

Data	Date
1. Microwave data	
TOPSAR data	3 December, 1996
2. Optical data	
SPOT-4	18 December, 2003
3. Topographic maps	
1:25,000 scale	1959
Ground survey	14- 27 August, 2003
	5-18 December, 2003

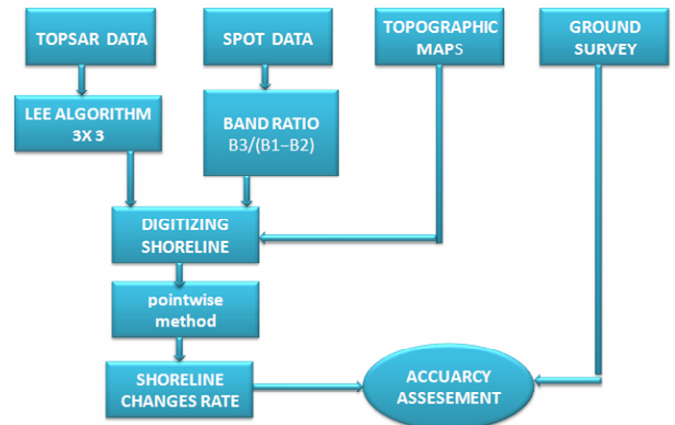


**Figure 1.** Block diagram for shoreline changes rate estimation.

EASI/PACE image processing system. By using projection techniques, the topographic map of 1959 of 1:25,000 scale, was rectified to the topographic map of 1:60,000 scale. Both multispectral SPOT, aerialphotographs and TOPSAR data, geocoded by using topographic map, to correct the geometric distortion in the digital images. 20 GCPs on each remote sensing images are selected for registration, with RMS error not more than 0.5. If the errors are found to be above the 0.5, the GCPs selection was repeated by adding or deleting the points to improve the accuracy of the registration. The first four control points were dispersed around the edges of the image to ensure the mapping polynomials are well-behaved over the image and other GCPs were dispersed along the study area to ensure the optimal accuracy of the image as suggested by Richards (1993) and Campbell (2002). The first degree polynomial registration was found to fit the transformation for the images.

**Ground survey**

The GPS survey used to: (i) to record exact geographical position of shoreline; (ii) to determine the cross sections of shore slopes; (iii) to verify the reliability of remote sensing georeferencing; and finally, (iv) to create a reference network for future surveys. The geometric location of the GPS survey was obtained by using the new satellite geodetic network, IGM95. After a careful analysis of the places and the identification of the reference vertexes, we thickened the network around such vertexes in order to perform the measurements for the cross sections (transects perpendicular to the coastline). The GPS data collected within 15 sample points

scattered along 30 km coastline with interval distance of 2 km between every sample locations. In every sample location, Rec-Alta (Recording Electronic Tacheometer) was used to acquire the beach profile ground truth data was collected on the August, 2003 which was before the north east monsoon period and December, 2003, during the North east monsoon season.

**shoreline changes rate estimation**

The vegetation line in the topographic maps and remote sensing data are digitized into the vector layer. Thus, the MHL water line does not consider in this study. According to Maged (2001), MHL water lines are in the dynamic cycle which mainly a source of inaccurate shoreline position. The remote sensing vectors were overlaid with the vectors of the topographic maps. On each data, location, which are well defined as such as road junctions were selected, the perpendicular line from the center of road junctions to shoreline is plotted. Then, the distance from the center of the junction to the point where the line and coastline intersect was determined. In order to estimate the shoreline changes rate, 30 transects are plotted perpendicular to shoreline to intercept the overlapped shoreline positions. These profiles are coincided with the similar location of sample ground survey points. The distance from each interception to the baseline was measured along these transects. Following Chien (2007), the pointwise method is applied to estimate shoreline changes rate. In doing so, the shoreline within a single cell sized  $\Delta X$  and  $\Delta Y$  has a unique orientation characterized by the angle  $\Phi$  (Figure 2). The retreat distance  $\Delta R$  in x-dimension is:

$$\Delta R_x = \Delta R \cos^{-1} \Phi \tag{2}$$

Along shoreline vector digitized polygone, points Y1 and Y2 has unlike retreat distances  $r_1$  and  $r_2$  and equal

$$r_1 + r_2 = 2 (\Delta R_x \cos^{-1} \Phi) \tag{3}$$

The following pseudocode was used to estimate the retreat position of shoreline:

```

-----
Input different period vector polygone layers of shoreline
For each time step do
Calculate retreat distance  $\Delta R$  for  $j=1,2,\dots,N_y$ ,
Calculate new position of shoreline  $r[i]=0.5 (\Delta R_{x_i} - r_{i-1})$ ,
End for
-----
    
```

**Accuracy assessment**

In this study, the significant difference test of statistical T-test is used to determine the performances of TOPSAR polarized bands. In addition, regression statistical linear also implemented to determine the correlation between ground survey and remote sensing data. Finally, root mean square of bias (RMSE) is used to determine the level of accuray of rates of shoreline changes from

TOPSAR data ( $R_{TOPSAR}$ ) comparing with ground survey ( $R_{Ground}$ ). The root mean square of bias equals

$$RMS = [N^{-1} \sum_{i=1}^N (R_{TOPSAR} - R_{Ground})^2]^{0.5} \tag{4}$$

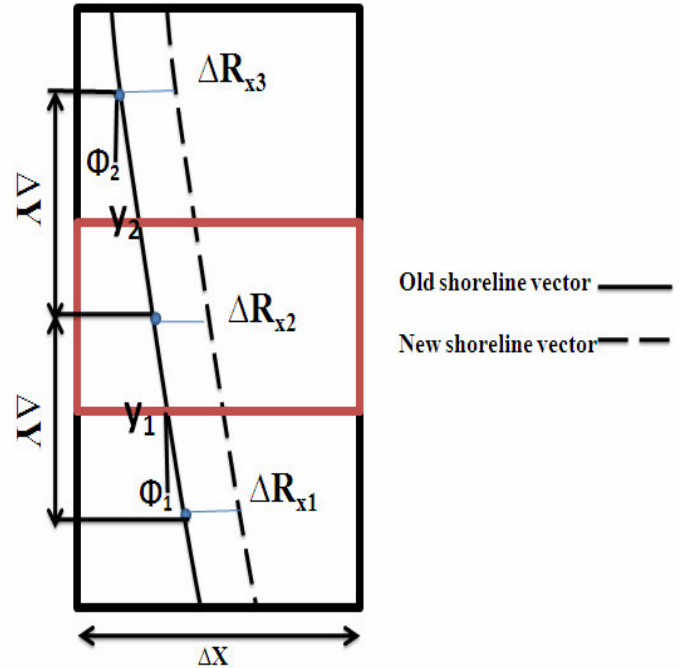


**Figure 2.** Pointwise method used for shoreline changes rate estimation.

where N is number of observations used to estimate RMSE.

**RESULTS AND DISCUSSION**

Figure 3 shows Lee algorithm results for different TOPSAR polarized bands. Obviously, Lee algorithm with kernel window size of 3x3 pixels has better performance in Cvv bands than  $L_{HH}$  and  $L_{VV}$  bands, respectively. Evidently, Cvv band has the lowest signal to noise ratio of 1.6. This allows for preserving the edge of linear infrastructure features such as roads and also shoreline boundary. According to Maged et al. (2010), Lee algorithm provides a way of edge detection for shoreline boundary as close to reality. This confirms the study of Maged (2002).

The coastline change rates modeled from the topographic map 1959 that was estimated from various TOPSAR (1996) polarized bands and then are compared to the SPOT satellite data (2003) with ground truth data which are observed in years 1996 and 2003 are shown in Figure 4. TOPSAR L-band HH and VV polarized images having a strong similarity while the change pattern in C-band image is dissimilar to the L-band. The T- test conducted with  $P < 0.05$  suggested that there are significant differences between L- and C-band in mapping the coastline change.

Table 2 shows that Cvv has lower RMSE value of  $\pm 0.9$  than  $L_{HH}$  and  $L_{VV}$ , respectively. This confirm the results of Figure 3. In addition, the stronger correlation is shown between Cvv, SPOT satellite data and ground data with

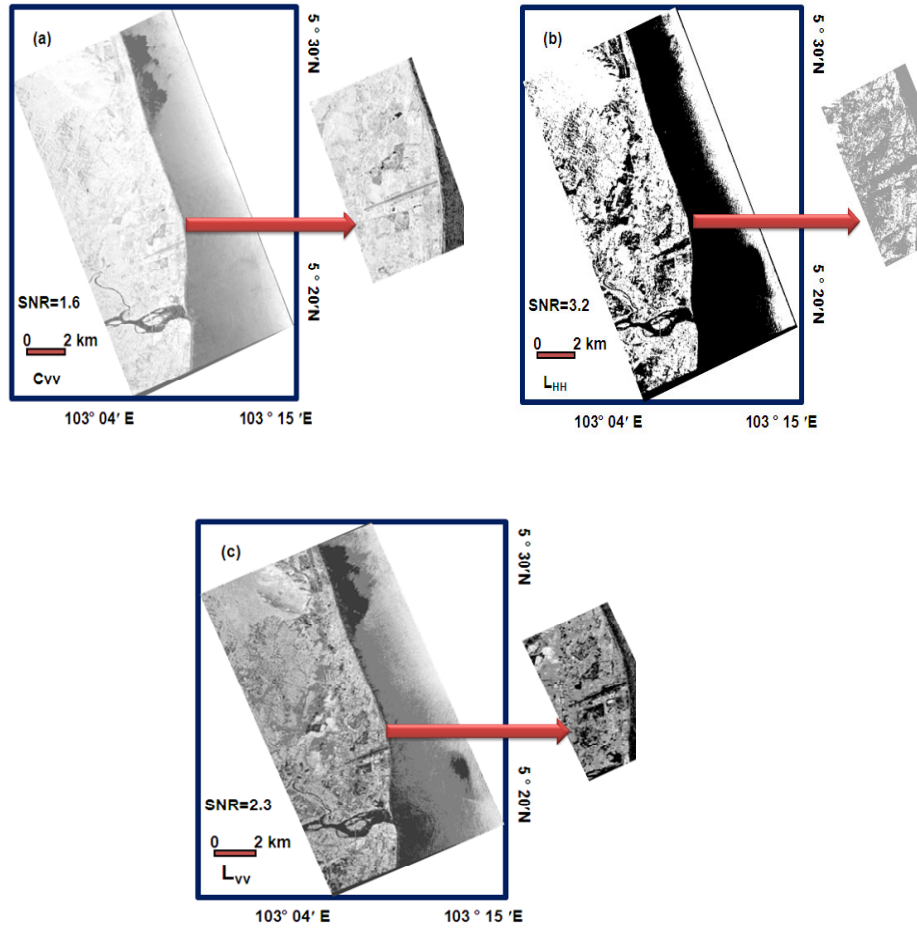


Figure 3. Lee algorithm results for (a) Cvv, (b) LHH, and (c) Lvv different TOPSAR polarized bands.

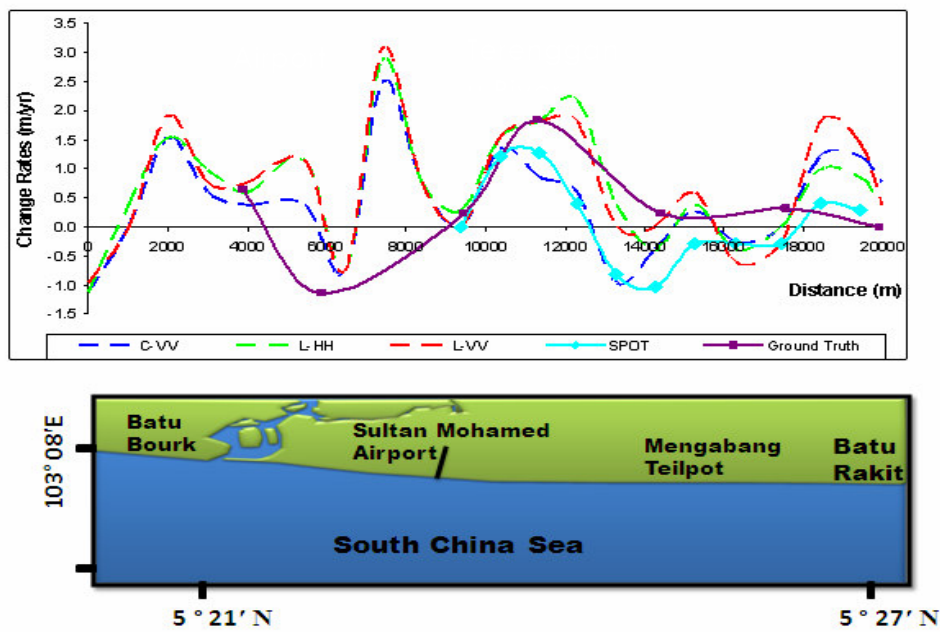


Figure 4. Output results of coastline change model.

**Table 2.** Regression model of TOPSAR comparisons.

TOPSAR Data	Correlation coefficient ( $R^2$ )		RMSE (m/yr)
	SPOT data	Ground data	
$C_{VV}$	0.71	0.73	$\pm 0.9$
$L_{HH}$	0.61	0.34	$\pm 2.0$
$L_{VV}$	0.66	0.43	$\pm 1.7$

$R^2$  of 0.71 and 0.73, respectively. This indicates that the RMSE is reduced with the integration between SPOT data and  $C_{VV}$  in comparison to  $L_{HH}$  and  $L_{VV}$  bands. In  $C_{VV}$  and near IR, the land-water interface is clearly defined as the water absorbed the radiation energy and, thereby, contributed nearly no energy returns in case of near IR. This result confirm the studies of Maged (2002) and Guariglia et al. (2006).

Discrepancy of L- and C-bands in mapping coastline change is very much related to the differences of backscattering in each TOPSAR band. Different bands in TOPSAR generate a radiation of different frequencies and wavelengths. The wavelength of L-band (24 cm) is varying to wavelength in C-band (6 cm). According to Short (2003), radar wavelengths influence penetrability below target tops to ground surface and depth of the penetration increases with wavelength. In this study, the coastline change was focused on the changes of vegetation cover along the coastline. In vegetation area, shorter wavelength such as C-band reflect mainly the first leaves encountered from the canopy tops. In C-band image, the vegetation covers are signified by brighter pixels as described by Freeman (1994) that the objects approximately the size of the wavelength appearing bright and objects smaller than wavelength appearing darker. L-band radar generates longer wavelength thus penetrate deeper. Most of the plant leaves are too small to have much influence on backscatter at longer wavelength. Longer wavelength easily penetrates through the vegetation cover, thus it is difficult to identify the coastline accurately in L-band image. This leads to the error interpreting in studying the image. Table 3 shows that there is significant relationship between  $C_{VV}$  band and  $L_{HH}$  and  $L_{VV}$  bands respectively. This is shown by P values of 0.031 and 0.006, respectively. This significant difference consider the source of error that has occurred between SPOT, ground survey and TOPSAR polarized bands (Table 2).

In general, the result of the study suggested that TOPSAR C-band could produce better image in mapping the coastline change. This can be proved by the comparison of the output result with SPOT and ground data. Table 2 shows that C-band result having a higher similarity to the change pattern of SPOT and ground data. The regression model shows both the L-band HH and VV images are not as capable for mapping coastline change as in C-band. Further, the change model in Figure 4 shows the increasing of the difference between

**Table 3.** Hypothesis test of significant difference.

Comparison	P-value	Relation
$C_{VV} - L_{HH}$	0.031	Significant difference
$C_{VV} - L_{VV}$	0.006	Significant difference
$L_{HH} - L_{VV}$	0.648	No significant difference

L and C-band at the area of sedimentation but this variation decrease at the area of erosion. In C-band image, digitization of vector was drawn exactly over the vegetation line along the coastal, as the vegetation cover and beach area can be well identified. In L-band image, the differences between vegetation cover and sandy area are not clearly interpreted, thus possibility of error digitization occurred, in which the vector was not drawn on vegetation line but on water edge which is in front of the vegetation cover. As a result, L-band shows a higher accretion rate in sedimentation area, due to expand of sandy beach and mistaken digitization on water edge. This error interpreting decrease at the erosion area as the water edge proceeds nearer to the vegetation line. The phase difference between HH and VV plays an important role in separating surface scattering, diffuse scattering and double bounce scattering. Randy et al. (1999) mentioned that HH polarization performs better and more consistently in detecting land cover features. The comparison of L-band HH and VV images shows that, HH polarized image is more suitable for mapping coastline change. This can be explained by Barrett and Curtis (1992) that vegetation response more to like-polarization.

## CONCLUSION

The study evaluates that there are significant differences that occurred among the TOPSAR L- and C-band image in mapping the coastline change. The C-band showed the potential to be the best polarized data that can be used in coastline change detection as it show the clearest image for easier coastline identification. In C-VV image, the shoreline, vegetation cover, and the sand bar can be finely detected after the application of linear contrast, Gaussian and histogram equalization algorithms. Comparison between HH and VV polarizations suggested that HH polarized data is more fitting for mapping the coastline change. Comparison with SPOT and ground data shows that the mapping results of TOPSAR are accurate. The study concluded that TOPSAR polarized C-band data are an excellent tool for mapping the coastline change.

## REFERENCES

- Anders FJ, Byrnes MR (1991). Accuracy of shoreline change rates as determined from map sand aerial photographs. *Shore and Beach*, 59:

17-26.

- Boak EH, Turner IL (2005). Shoreline definition and detection: a review. *J. Coastal Res.*, 21: 688-703.
- Barrett EC, Curtis LF (1992). Introduction to environmental remote sensing, 3<sup>rd</sup> edition. Chapman and Hall, p. 426.
- Campbell JB (2002). Introduction to remote sensing, third edition. The Guilford Press, New York p. 620.
- Chien NQ (2007). Simulating shoreline retreat in a 2-D hydro-morphologic model. Msc. Theses, Institute of UNESCO-IHE for water education, Delft, The Netherlands.
- El-Raey MSM, Nasr MM, El-Hattab (1995). Change Detection of Rosetta promontory over the Last Forty Years. *Int. J. Remote Sensing*, 16(5): 825-834.
- Guariglia A, Buonamassa A, Losurdo A, Saladino R, Trivigno ML, Zaccagnino A, Colangelo A (2006). A multisource approach for coastline mapping and identification of shoreline changes. *Ann. Geophys*, 49(1): 295-304.
- Freeman T (1994). What is imaging radar? Jet Propulsion Laboratory [online]. <http://trfic.jpl.nasa.gov/GRFM/cdrom/africa/docs/html/imgv3.htm> [Accessed 17 July 2003].
- Frihy OE, Nasr SM, El Hatab MM, El Raey M (1995). Remote sensing of Beach Erosion Along the Rosetta Promontory, Northwestern Nile delta, Egypt. *Int. J. Remote Sens.*, 15(8): 1649-1660.
- Gens R (2010). Remote sensing of coastlines: detection, extraction and monitoring. *Int. J. Remote Sens.*, 31(10): 1819-1836.
- Kim DJ, Moon WM, Park SE, Kim JE, Lee HS (2007). Dependence of waterline Mapping on radar frequency used for SAR images in intertidal areas. *IEEE Geosci. Remote Sens. Lett.*, 4: 269-273.
- Lee JS, Jurkevich I (1990). Coastline detection and tracing in SAR images. *IEEE Transact. Geosci. Remote Sens.*, 28: 662-668.
- Liu H, Jezek KC (2004). Automated Extraction of Coastline from Satellite Imagery by Integration Canny Edge Detection and Locally Adaptive Thresholding Methods. *Int. J. Remote Sens.*, 35: 973-958.
- Maged MM (1999). A method for Wave Spectra Refraction Analysis by TOPSAR Polarized Data. IGARSS '99 28 June-2 July 1999, Hamburg, Germany, 2: 2343-2346.
- Maged M (2000). Operationalisation Model of Coastal Erosion Studies by SAR Polarised Data. *J. GIS@Development*, 4(8): 17-20.
- Maged M (2001). Operational of Canny algorithm on SAR data for modeling shoreline change. *Photogrammetrie Fernerkundung Geoinfo. Germany*, 2: 93-102.
- Maged M (2001). A comparison between quasi-linear and Velocity Bunching Models for Modelling Shoreline Change. *Asian J. Geoinfo.* 2(2): 3-14.
- Maged M (2001). TOPSAR wave spectra model and coastal erosion detection. *Intl. J. Appl. Earth Observ. Geoinfo. Elsevier*, 3(4): 357-365.
- Maged M, Hashim M (2006). Three-Dimensional Reconstruction of bathymetry Using C-Band TOPSAR. Data. *Photogrammetrie Fernerkundung Geoinformation*. 6/2006, S. 469-480.
- Maged M, Sabu Z, Hashim M (2010). Mapping coastal geomorphology changes using Synthetic Aperture Radar data. Paper submitted to *Int. J. Phy. Sci.*, pp. 5(12): 1890-1896.
- Melba M, Kumar S, Richard MR, Gibeaut JC, Amy N (1999). Fusion of Airborne polarimetric and interferometric SAR for classification of coastal environments. *IEEE Transactions Geosci. Remote Sens.*, 37: 1306-1315.
- Pajak MJ, Leatherman S (2002). The high water line as shoreline indicator. *J. Coastal Res.*, 18: 329-337.
- Randy JNV, Paringit EC, Lopez ED (1999). Discriminant analysis of polarimetric SAR data for coastal land cover feature detection. *ACRS* [online]. <http://www.gisdevelopment.net/aars/acrs/1999/ps4/ps400c.shtml> [Accessed 17 July 2003].
- Richards JA (1993). Remote sensing digital image analysis. Springer-Verlag Berlin Heidelberg, Germany, p. 340.
- Short NM (2003). Remote sensing tutorial. Goddard Space Flight Center, NASA [online]. <http://rseol.gsfc.nasa.gov/RSTutorial/Front/overview.html> [Accessed 17 July 2003].
- Stocdon HF, Sallenger AH, list JH, Holman RA (2002). Estimation of shoreline Position and change using airborne topographic lidar data. *J. Coastal Res.*, 18: 502-513.
- Shu Y, Li J, Gomes G (2010). Shoreline extraction from RADARSAT-2 intensity imagery using a narrow band level set segmentation approach. *Marine Geodesy*, 33: 187-203.
- Teodoro AC, Barbosa JP, Gomes FV, Pinto FT (2009). Evaluation of beach hydromorphological behaviour and classification using image classification techniques. *J. Coastal Res.*, 56: 1607-1661.
- Yu Y, Acton ST (2004). Automated delineation of coastline from polarimetric SAR imagery. *Int. J. Remote Sens.*, 25: 3423-3438.